JOURNAL OF GEOPHYSICAL RESEARCH, VOL. 106, NO. D20, PAGES 24,107–24,117, OCTOBER 27, 2001

Measurements of enhanced H_2SO_4 and 3-4 nm particles near a frontal cloud during the First Aerosol Characterization Experiment (ACE 1)

R. J. Weber,[1] G. Chen,[1] D. D. Davis,[1] R. L. Mauldin III,[2] D. J. Tanner,[2] F. L. Eisele,[1,2] A. D. Clarke,[3] D. C. Thornton,[4] and A. R. Bandy[4]

Abstract. Observations of new particle production recorded near a frontal cloud at ~6 km above sea level in a remote marine region are reported. Two distinct locations situated near the cloud were found to have enhanced concentrations of sulfuric acid vapor (H_2SO_4) and freshly formed 3-4 nm particles. Both were in droplet-free air situated above cloudy regions. No evidence for enhanced H_2SO_4 or nucleation was observed in clear air far from the cloud. In the nucleating region the aerosol size distribution from 3 nm to 600 μm was observed to be trimodal, with a prominent ultrafine mode, and was qualitatively similar to surface-based measurements recorded in regions of postfrontal subsidence. The measurements support the notion that new particle production in the free troposphere occurs preferentially in clear air near clouds via enhanced photochemical production of nucleation precursor gases and that H_2SO_4 participates. A model simulation suggested that a doubling of ultraviolet intensities above the cloud due to cloud enhanced up-welling radiation or reasonable enhancements in sulfur dioxide concentrations could account for the higher H_2SO_4 concentration observed near the cloud. In the nucleation regions, H_2SO_4 and water vapor concentrations were too low for binary nucleation of sulfuric acid and water, according to current nucleation models. The mechanisms of particle formation and growth remain uncertain. The measurements were part of the first Aerosol Characterization Experiment (ACE 1) conducted in the remote South Pacific Ocean (153°E, 47°S) on November 27, 1995.

1. Background

Non-sea-salt sulfate particles in the remote marine boundary layer (MBL) may affect global climate through their influence on the Earth's radiation balance by directly scattering radiation and indirectly by serving as cloud condensation nuclei [*Coakley et al.*, 1983; *Fouquart and Isaka*, 1992]. Both models [*Capaldo et al.*, 1999; *Katoshevski et al.*, 1999; *Raes*, 1995] and measurements [*Clarke*, 1992; *Clarke et al.*, 1998; *Covert et al.*, 1996] suggest that a significant portion of the MBL non-sea-salt sulfate particles are formed in the free troposphere and entrained into the MBL by mixing processes. Evidence of this has been observed in regions of postfrontal subsidence as a distinct MBL ultrafine particle mode between 3 and 20 nm [*Covert et al.*, 1996]. Under more typical conditions, this mode is rarely observed in the remote marine boundary layer.

Recent studies have shown that a major source of free-tropospheric nanoparticles is associated with particle production in regions near clouds [*Clarke et al.*, 1999; *Clarke et al.*, 1998]. The first Aerosol Characterization Experiment (ACE 1) provided further support for these observations. Regions of high 3-10 nm particle concentrations were often observed associated with clouds at altitudes ranging from ~2 km above sea level (asl) to an upper measurement range of ~6 km asl. Because concentrations of these particles were observed to peak near midday, they appear to be derived from photochemical processes [*Clarke et al.*, 1998].

These findings generally support earlier observations of particle formation in regions of cloud venting [*Hegg et al.*, 1990; *Perry and Hobbs*, 1994]. Models, based on observations, suggested that new particles were formed in these regions via binary H_2SO_4-H_2O nucleation [*Hegg et al.*, 1990; *Perry and Hobbs*, 1994]. The upper perimeters of convective clouds appear to be ideal sites for new particle production due to enhanced actinic fluxes, high relative humidity fields, cold temperatures, and reduced aerosol surface areas associated with higher altitudes. High actinic fluxes from down-welling and cloud reflected up-welling radiation combined with enhanced water vapor concentration could lead to increased photochemical production of OH, which in turn leads to production of low volatility products, such as H_2SO_4 production from sulfur dioxide (SO_2) oxidation. Measurements of high OH concentrations above

[1]School of Earth and Atmospheric Sciences, Georgia Institute of Technology, Atlanta, USA.
[2]Atmospheric Chemistry Division, National Center for Atmospheric Research, Boulder, Colorado, USA.
[3]School of Ocean and Earth Science and Technology, University of Hawaii at Manoa, Honolulu, USA.
[4]Department of Chemistry, Drexel University, Philadelphia, Pennsylvania, USA.

Paper number 2000JD000109.
0148-0227/01/2000JD000109$09.00

clouds have been attributed to this phenomenon [*Mauldin et al.*, 1997]. Cold temperatures promote supersaturation (sulfuric relative acidity) of nucleation precursor vapors necessary for particle formation. New particle formation is also promoted in regions of reduced preexisting aerosol concentrations by reducing heterogeneous scavenging of precursor vapors and the newly formed particles. Cloud processing of aerosols may lead to reductions in aerosol surface area concentrations. *Perry and Hobbs* [1994] measured nucleation in outflow regions of a precipitating cloud where the aerosol surface area was low. Another factor that is thought to contribute to nucleation in these regions is enhancements of nucleation precursor species by convective lofting from the MBL, such as transport of dimethyl sulfide (DMS) from the surface to cloud venting regions leading to higher SO_2 and thus H_2SO_4 concentrations. Combined, these processes could produce conditions where binary H_2SO_4-H_2O nucleation is favored.

Depending on the prevalence of various precursor species, other photochemically induced nucleation mechanisms are possible, such as ternary H_2SO_4-NH_3-H_2O nucleation, or nucleation of organic species, possibly with H_2SO_4 also playing a role. Nucleation of H_2SO_4 ion clusters has also been proposed as a viable route for new particle production [*Turco et al.*, 1998]. All of these mechanisms would be consistent with observations of elevated H_2SO_4 concentrations in regions of particle formation. Other methods of particle production that do not necessarily depend on enhanced precursor concentrations have been proposed. For example, mixing processes along cloud perimeters may lead to particle production in these regions [*Nilsson and Kulmala*, 1998]. In this case, saturated H_2SO_4 conditions are reached not by the physicochemical dynamics between photochemical production and heterogeneous loss of precursor vapors but by mixing warm air at high relative humidity with colder dryer air. It has also been suggested that fragmentation of evaporating cloud drops could be a source of new particles near clouds [see *DeFelice and Cheng*, 1998, and references therein]. At this time the nucleation mechanism is not clear. Our analysis of measurements in near-cloud nucleation regions recorded during other flights of this study, however, show that the conditions were in fair agreement with those predicted by the *Jaecker-Voirol and Mirabel* [1989] binary H_2SO_4-H_2O model to be necessary for nucleation [*Clarke et al.*, 1999; *Weber et al.*, 1999b]. The data were inconsistent with particle formation due to fragmenting cloud drops [*Weber et al.*, 1998a].

2. Observations: Evidence of Nucleation Near a Frontal Cloud

During the first Aerosol Characterization Experiment (ACE 1) intensive operations, airborne measurements with the National Center for Atmospheric Research (NCAR) C-130 aircraft were based at Hobart, Tasmania, Australia. One flight (research flight 16) was committed to making measurements in the vicinity of Macquarie Island (54.5°S, 159°E) for intercomparisons with ground-based measurements [*Weber et al.*, 1999a]. During the ferry flight to Hobart, a cloudbank associated with a southerly moving cold front was intercepted. Figure 1 shows the National Oceanic and Atmospheric Association (NOAA) infrared satellite image (NOAA-12 IR channel 4) taken on November 27, 1995, at 0439 UTC, approximately 1 hour before the aircraft penetrated the cloud on the return flight from Macquarie Island. The approximate flight path on the return leg is also shown in Figure 1.

2.1. Meteorological Measurements Near the Cloud

Airborne measurements of cloud water/ice concentrations, relative humidity, aircraft altitude, ambient temperature, and down-welling and up-welling short-wave radiation recorded in the vicinity of the frontal cloud are shown in Figure 2. Measurements of various gas and aerosol particles are shown in Figure 3. For descriptions of the various airborne instruments, see the ACE 1 special section and accompanying papers [i.e., *Bates et al.*, 1998].

Periods of in-cloud sampling can be identified from cloud droplet/ice concentrations (~2.0 - 47 μm diameter particles) measured by a wing-mounted forward scattering spectrometer probe (FSSP-100, PMS, Boulder, Colorado). From the cloud droplet data shown in Figure 2a, the aircraft entered the main part of the frontal cloud at about 0522 UTC, and exited it at approximately 0551 UTC, corresponding to local Sun times (LST, Sun reaches zenith at 1200) of 1522 and 1551, respectively. The approximate aircraft position at various times, including entering and leaving the frontal cloud, are shown on the satellite image in Figure 1. The area between the shaded regions in the plots of Figures 2 and 3 are sampling periods within the main cloud. The shaded regions on each plot identify locations of high 3-4 nm particle concentrations and are indicative of recent particle production. This will be discussed further in the following sections.

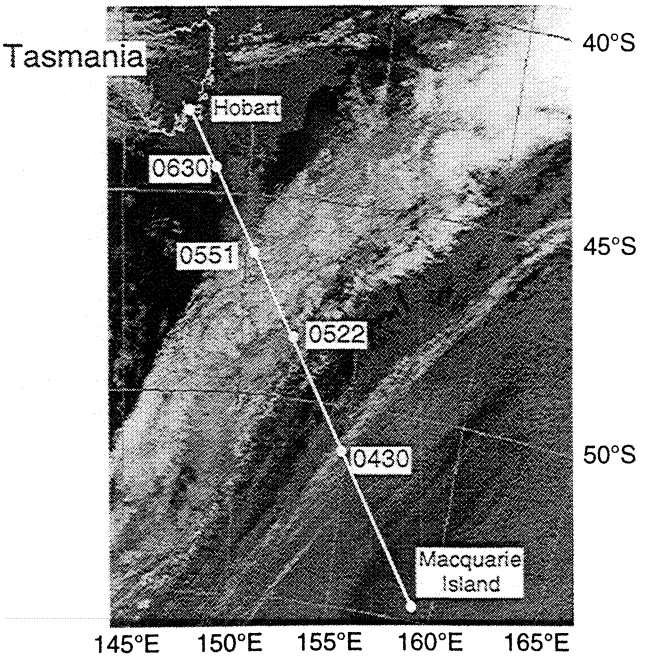

Figure 1. IR satellite image of a frontal cloud and approximate flight path of the C-130 research aircraft during transit from Macquarie Island to Hobart, Tasmania, Australia, on November 27, 1995 (J.D. 331). The aircraft approximate position at various times is also shown.

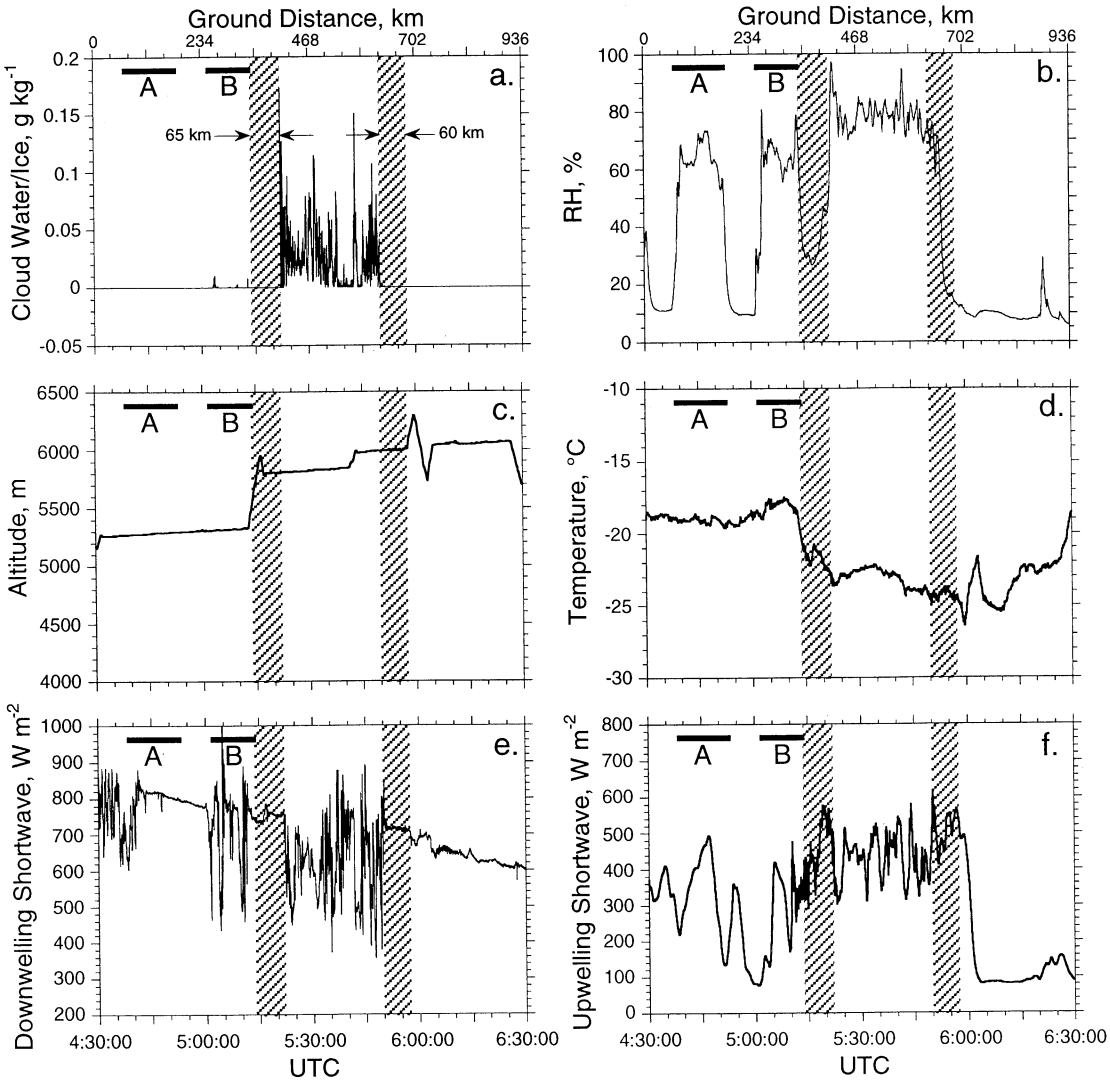

Figure 2. Plots of various parameters measured in the vicinity of the frontal cloud shown in Figure 1. The shaded areas indicate nucleation regions where high 3-4 nm particle concentrations were recorded. The region between the shading is a period when we were sampling within the frontal cloud. Horizontal bands labeled A and B identify the two regions of high RH encountered prior to entering the frontal cloud. The approximate distance the aircraft traveled relative to the start of the interval plotted is shown at the top of Figures 2a and 2b using an average ground speed of 130 m s^{-1}.

Figure 2b shows the measured relative humidity (RH). In the time interval plotted, three distinct RH peaks were recorded. The first two high-RH regions are identified in all plots in Figures 2 and 3 by bands labeled A and B. Note that in the high-RH region B some cloud droplets were detected (Figure 2a). This is significant because measured OH concentrations were high in this region but sulfuric acid concentrations were low, likely due to scavenging by the droplets since the characteristic lifetime of a H_2SO_4 molecule due to scavenging in this region is calculated to be only about 4 min. This is based on the Fuchs-Sutugin factor determined from the measured aerosol size distribution [*Fuchs and Sutugin*, 1970]. Thus nucleation is not expected within this cloud due to limited H_2SO_4 concentrations. The primary region of high RH was within the main cloud where the RH ranged from 80 to near 100% and dropped off rapidly along the cloud perimeter to 10-30%. Note that although this change in RH along the cloud perimeter appears as a rapid decrease in the plot, the precipitous change in Figure 2b from ~70 to 18% RH after exiting the cloud (~0554 UTC) actually spans a measurement interval of ~136 s. At an average aircraft speed of about 130 m s^{-1}, this corresponds to a distance of ~20 km. Thus the drop in RH with increasing distance from the cloud is fairly gradual with an average gradient of roughly 3% drop in RH per kilometer. The two other RH peaks were observed prior to entering the main cloud between 0440 and 0452 (labeled A in Figures 2, 3, 4 and 6), and 0503 and 0513 UTC (labeled B).

Measured down-welling short-wave radiation shown in Figure 2c was uniformly high in the nucleation regions adjacent to the frontal cloud, indicating clear sky above. However, in regions where cloud droplets were detected (high-RH region B and within the main frontal cloud) the down-welling short-wave radiation was highly variable. Up-welling radiation was significantly higher in the nucleation regions, consistent with the video images showing that the

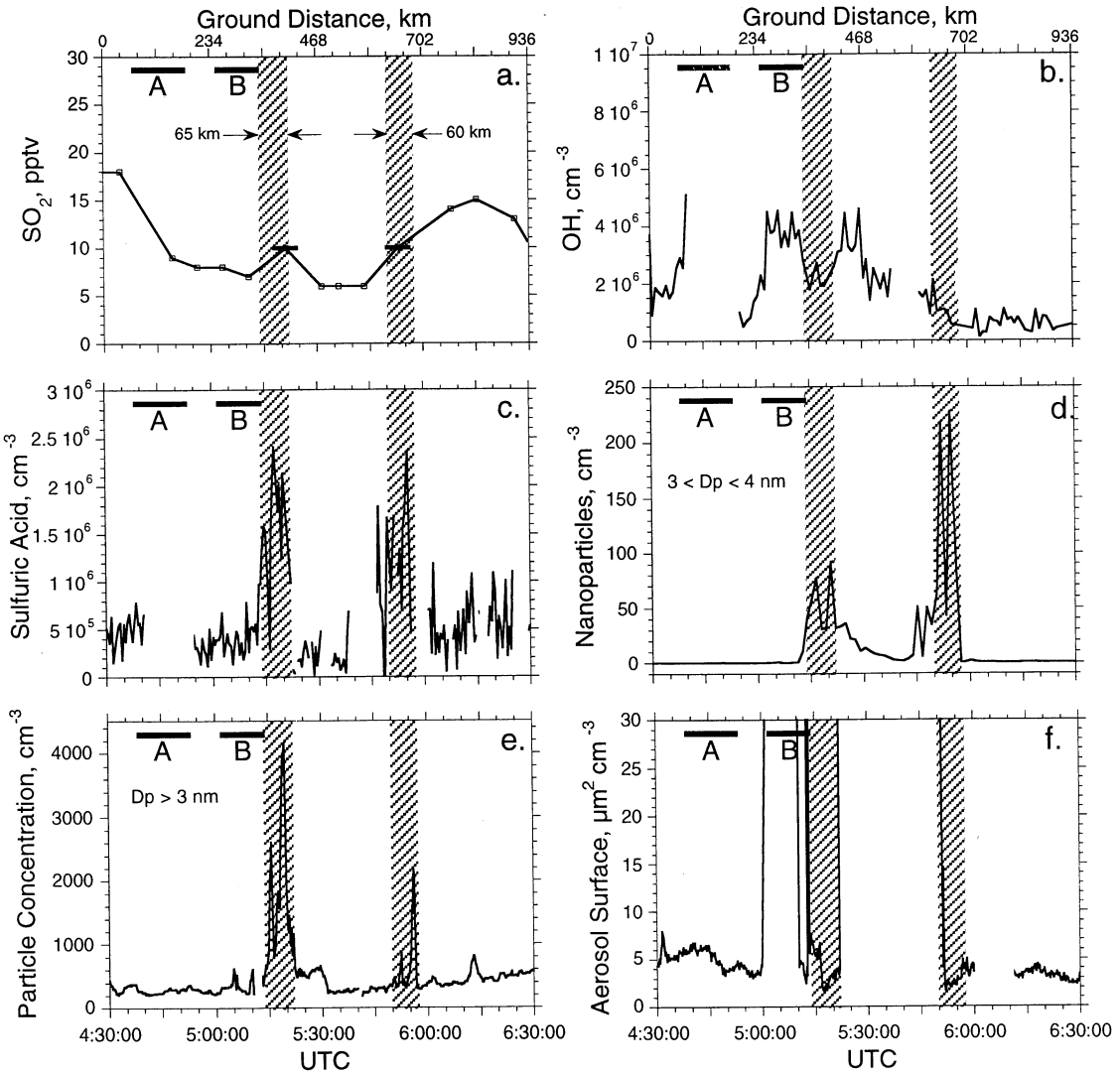

Figure 3. Same as Figure 2, but plots of species pertinent to studies of new particle formation in the vicinity of the cloud.

cloud extended below the aircraft in these regions. This would explain the higher up-welling short-wave radiation extending farther out from the region containing the cloud droplets and corresponds to the region entering and exiting the main frontal cloud where 3-4 nm particles were detected. The satellite image in Figure 1 also shows the cloud extending farther out on either side of the cloud penetration region, shown as the period between 0522 and 0551. In addition, the satellite image shows evidence of cloud ribbons running parallel to the main cloud, consistent with the observation of higher RH bands near the main cloud. A schematic diagram showing the aircraft flight path relative to the clouds, consistent with these observations, is shown in Figure 4. The measurements suggest that we were passing in and out of regions of varying cloudiness prior to entering the main frontal cloud and that we traversed the top section of the frontal cloud.

2.2. Gas and Aerosol Measurements Near the Cloud

Measurements of SO_2, OH, H_2SO_4, freshly formed 3-4 nm diameter particles, total CN, and aerosol surface area concentrations recorded near the frontal cloud are plotted in Figure 3. In Figure 3a, SO_2 concentrations are not significantly higher in the near-cloud nucleation regions. The time resolution of the SO_2 measurement, however, was the lowest of all measurements at 6 min integrated averages. The SO_2 measurement interval in the nucleation region is shown as a bar. OH concentrations, shown in Figure 3b, are also not significantly higher in the nucleation regions; however, OH concentrations were higher in the high-RH region B. Figure 3c shows that H_2SO_4 was most abundant in the nucleation regions along both sides of the cloud perimeter where up-welling radiation was greatest. In these regions, acid concentrations ranged from 1.5×10^6 to 2.5×10^6 cm^{-3}. The peak concentrations are about 5 times higher than levels farther away, and about 2 to 3 times higher than the average concentration of 8×10^5 cm^{-3}, observed at this altitude during the ferry flights to and from Macquarie Island. The measurements suggest that H_2SO_4 was generated preferentially in regions above the frontal cloud. Figure 3c also shows that H_2SO_4 concentrations were very low in the high-RH region B, despite elevated OH concentrations and similar SO_2 concentrations. This may be explained by the

much higher aerosol surface area concentrations in this region (surface area concentrations are shown in Figure 3f).

In precisely the same locations of high H_2SO_4, concentrations of nominally 3-4 nm particles and total condensation nuclei (UCN, all particles larger than 3 nm) were also much higher, suggesting that new particle formation had occurred in these two regions. UCN concentrations were about 5 to 6 times higher in these regions compared to background levels. For the free tropospheric duration of this flight, the measurements near the cloud are the only regions where significant particle production was observed.

Figure 3d shows that we recorded nonzero concentrations of 3-4 nm particles within the cloud. We view these measurements as unreliable due to the likelihood of spurious particles created from shattering of cloud droplets with aerosol inlet sampling surfaces [*Weber et al.*, 1998a]. Earlier work, however, has suggested that nucleation may occur within clouds [*Hegg*, 1991]. In this case nucleation seems unlikely in the cloud due to the high aerosol surface areas in this region (Figure 2f, the area is off scale but of the order of 10^3 μm^2 cm^{-3}). Despite this we note that just prior to exiting the cloud a region of higher sulfuric acid concentrations was detected. There is little sulfuric acid data within the cloud because the instrument is generally shut down since liquid water renders the instrument inoperable. Thus as with the particles, the acid concentrations measured in the cloud must be viewed with some skepticism. It is also noted that in Figure 3 there is a correlation between the in-cloud sulfuric acid peak and 3-4 nm particles, but that there is no enhancement in the total UCN. These measurements are from a region in the cloud of consistently high cloud water/ice concentrations where sampling artifacts are more likely (Figure 2a). At this point we make no conclusions on nucleation within the cloud due to the unreliability of the in-cloud data.

The possibility of droplet shatter as a source for the observed peaks in particle concentrations adjacent to the cloud is ruled out since no cloud droplets were recorded in these regions. Moreover, measurements of refractory CN (CN that survive heating to 300°C) indicated that primarily all of the particles comprising the UCN peaks in the nucleation region were volatile. Our work has shown that spurious UCN measurements from droplet shatter are highly correlated with liquid water concentrations, and in marine regions, shattered droplets usually contain refractory material (e.g., sea salt) [*Clarke et al.*, 1997; *Weber et al.*, 1998a].

The aerosol surface area is shown in Figure 3f. This is based on the combined size distributions measured by a differential mobility analyzer ($0.01 < Dp < 0.16$ μm) [*Knutson and Whitby*, 1975] and a combination of optical probes spanning diameters from 0.18 to 400 μm (PCASP, FSSP-300, FSSP-100, and 260-X, all PMS probes, Boulder Colorado). Measurements are adjusted to ambient RH assuming particle water uptake is as pure H_2SO_4 aerosol. Periods of high particle surface areas (off scale in Figure 3f) are regions containing droplets. Two regions of high surface areas were encountered: the area identified as within the frontal cloud and also the RH peak B encountered just prior to entering the main cloud. In clear air near the cloud, aerosol surface areas ranged from about 3 to 8 μm^2 cm^{-3}, similar or slightly lower than concentrations measured in clear air at this altitude. Thus surface areas were not dramatically lower in the region near the cloud where nucleation was observed.

2.3. Aerosol Size Distributions Near the Cloud

The aerosol number distribution corresponding to the highest nanoparticle concentration (0554 UTC) in the nucleation regions is shown in Figure 5. Other distributions recorded in the nucleation regions were similar. In all cases the distributions peaked between 4 and 5 nm with only the concentration of the 3-10 nm mode differing. In other nucleation studies we have observed the distributions peaking at much lower sizes [*Weber et al.*, 1998b]. In this case most of the observed newly formed particles may have been produced earlier in the day and the particles were somewhat aged having had time to grow to larger sizes.

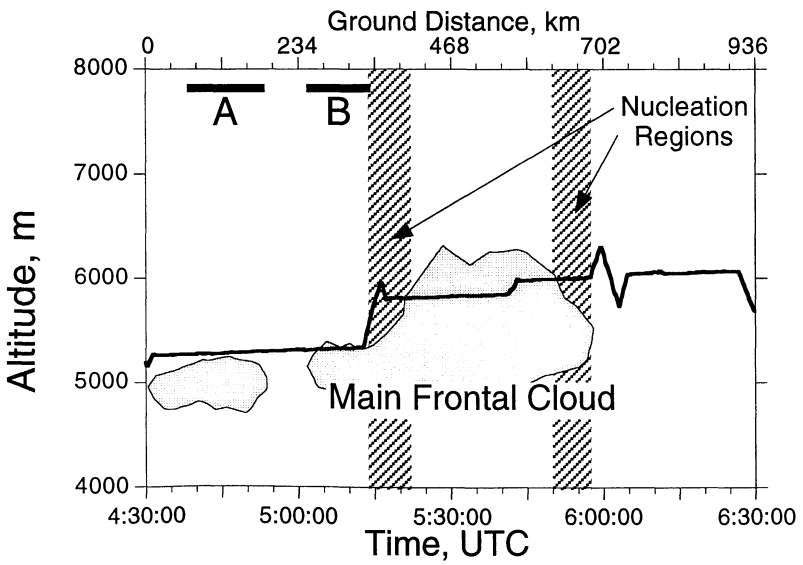

Figure 4. Schematic of aircraft position relative to the frontal cloud consistent with measurements of cloud droplets, up-welling and down-welling radiation (see Figure 2), the aircraft down-viewing video camera, and the satellite image (Figure 1). The approximate distance traveled by the aircraft is also given.

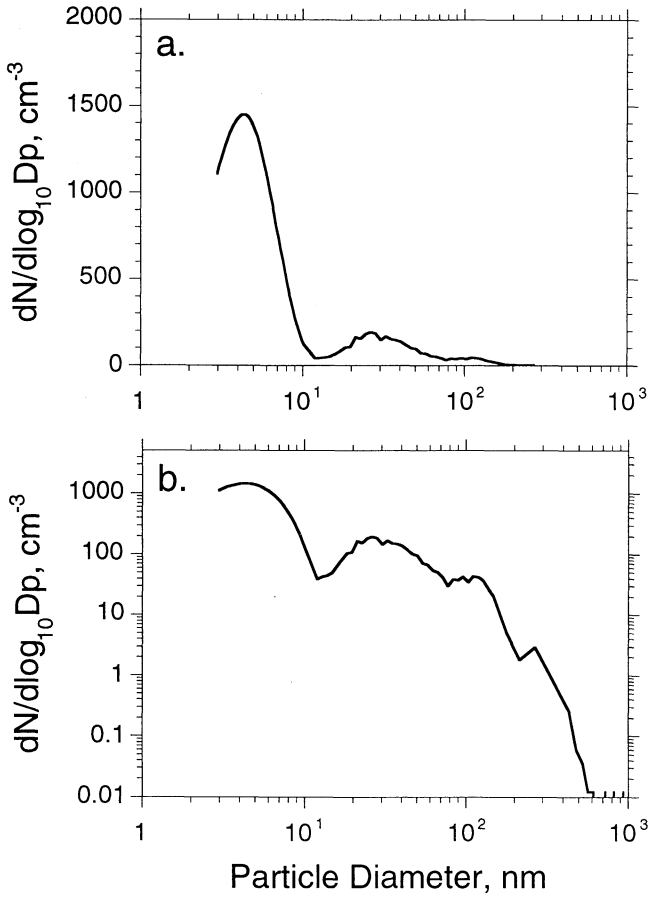

Figure 5. Example of the aerosol size distribution recorded near the cloud perimeter in the region of recent new particle production (0555 UTC) plotted on (a) linear and (b) logarithmic particle concentration scales.

On the transit to Macquarie Island in the morning at about 2300 UTC (0900 LST) the aircraft passed through a frontal cloud at a similar altitude (5.8 km) and location as on the return flight. Enhanced nanoparticle concentrations were observed within the cloud (likely an artifact), but no enhancements in H_2SO_4 or 3-4 particles were observed in the immediate vicinity of the cloud. If these nucleation regions occur over extended areas in the vicinity of the frontal cloud, then this lack of enhancements on the first transit flight would set a time limit on the age of the H_2SO_4 and nanoparticles to less than roughly 7 hours.

3. Discussion

The data support the hypothesis that photochemistry is a driving force for nucleation near clouds and that H_2SO_4 is a precursor. The measurements, however, do not readily suggest what produced the enhanced H_2SO_4 concentrations or help resolve the mechanism for particle formation.

Correlations between H_2SO_4 and nanoparticle concentrations are consistent with the view that nucleation processes involving H_2SO_4 formed these particles. Of interest is what produced the high H_2SO_4 concentrations and what mechanism lead to particle production. The peaks in H_2SO_4, nanoparticle and total particle concentrations were observed roughly 35 and 40 km from the southern (0522 UTC) and northern (0551 UTC) edges of the cloud perimeter, respectively, and each extended about 60 km from the edge of the cloud. In this case it seems most plausible that the nucleation regions are associated with clouds situated below the aircraft and which may have produce regions of enhanced photochemistry from higher actinic fluxes (down-welling plus up-welling radiation, Figures 2e and 2f). Note that highest H_2SO_4 concentrations were also confined to regions of droplet-free air (low surface area concentrations). Other factors may also play a role, such as additional precursor species and dynamic processes.

Focusing on the measurements prior to entering the main cloud (region B to within the main cloud) suggests that OH is anticorrelated with the H_2SO_4 and 3-4 nm particle concentrations. Note in Figure 3 that OH is high and H_2SO_4 low within the clouds, and OH is low and H_2SO_4 high in the droplet free region in between. This does not necessarily mean that OH played no role in the production of H_2SO_4. The data could be explained in the following way. Measurements of OH concentrations within clouds and above clouds have shown that high concentrations can be observed both in and above clouds [*Mauldin et al.*, 1997]. In this case, the two in-cloud regions had higher OH concentrations than the droplet free nucleation region in between. Sulfuric acid and 3-4 nm particle concentrations, however, could be lower in clouds due to scavenging by the drops. Combined, this leads to an anticorrelation between OH and H_2SO_4 when these limited in-cloud and above-cloud data are compared. A gas phase model simulation was carried out to help understand the possible causes for enhanced H_2SO_4 concentrations near the frontal cloud.

3.1. Gas/Aerosol Model Simulations

A number of mechanisms that could lead to enhanced H_2SO_4 concentration near clouds have been proposed, including increased photochemical production due to enhancements in both water vapor concentrations and UV intensities which result in higher OH concentrations. Enhancements in SO_2 concentrations from cloud pumping and venting of DMS with rapid conversion to SO_2. And finally, reduction in H_2SO_4 loss by preexisting particle scavenging due to a reduction of the aerosol surface area of preexisting particles due to cloud processing.

We have preformed a model simulation to test the sensitivity of H_2SO_4 production to OH enhancements. The hypothesis is that the reaction of SO_2 and OH served as the major source for H_2SO_4 and that the ambient H_2SO_4 concentrations are determined by a competition between H_2SO_4 production and loss by condensation onto preexisting particles and the production of new particles. We test if elevated H_2SO_4 concentrations, compared to clear-sky concentrations far from the cloud, could be explained by reasonable enhancements in OH production due to higher UV intensities above the cloud. We focus first on this mechanism because the observations show that SO_2 and aerosol surface area concentrations in the nucleation region were fairly similar to clear-sky concentrations and that short-wave radiation levels, due to greater up-welling radiation, was higher in the nucleation region. Short-wave radiation is used as a qualitative proxy for UV since no Eppley UV data were available during these measurements. Following this

analysis, the sensitivity of H_2SO_4 to SO_2 concentrations is explored.

3.1.1. Model. The photochemical model employed contains full HO_x-NO_x-methane chemistry, nonmethane hydrocarbon chemistry, and 14 sulfur chemistry reactions [*Davis et al.*, 1999]. The model is constrained by observations of other pertinent parameters. The photolysis rate coefficients are initially calculated using a National Center for Atmospheric Research (NCAR) Tropospheric Ultraviolet-Visible radiative transfer model for the clear-sky conditions and then multiplied by a cloud correction factor (CCF) to account for the sampling cloud conditions. The CCF is typically evaluated from the in situ UV observations (for a detailed discussion, see *Crawford et al.* [1999]). In this study, due to lack of UV measurements, the cloud correction factor was set up as an adjustable parameter to best fit the observed OH values. The output of the photochemical model includes a diel OH profile that can be used in H_2SO_4 calculation. Diurnal H_2SO_4 profiles were then calculated assuming initial concentrations of 10^3 cm^{-3} at 9:00 AM LST and using a constant preexisting aerosol scavenging factor of 5.7×10^{-5} s^{-1}, determined from the measured aerosol size distribution [*Fuchs and Sutugin*, 1970]. H_2SO_4 loss from the production of new particles was also considered in a rudimentary way. The 3-10 nm aerosol size distribution in the nucleation region, shown in Figure 5, was used to calculate the aerosol volume concentrations. Combined with the calculated H_2SO_4 hydration, we estimated that the production of these particles occurred over roughly a 4 hour period, which results in a H_2SO_4 loss rate of 40 H_2SO_4 molecules cm^{-3} s^{-1}. This is about a third of what is lost by scavenging onto the preexisting particles. This loss factor is introduced at 1000 LST and ramped up linearly to 40 cm^{-3} s^{-1} over a 1 hour period. This simplistic approach will tend to smooth out the temporal variation in H_2SO_4 if new particles are formed by a mechanism that is highly sensitive to the H_2SO_4 concentration, such as binary H_2SO_4/H_2O nucleation. We do not use a more sophisticated approach since the nucleation mechanism is unknown. The model also assumed a constant SO_2 concentration at the observed level of ~ 10 pptv. In the final model simulations the sensitivity of predicted H_2SO_4 concentrations to SO_2 was explored by increasing SO_2 concentrations to 17.5 pptv, the highest observed in the vicinity of the cloud (see Figure 3a).

3.1.2. OH simulations. Figure 3b shows that measured OH levels in the nucleation regions were not significantly enhanced: however, enhancements may have occurred earlier in the day when H_2SO_4 concentrations were being built up. Recall these measurements were made at local times between 1530 to 1600 LST. An interesting feature of the OH measurements is the region of high OH concentrations observed near the nucleation regions (B on Figures 2, 3, and 4) but with no corresponding H_2SO_4 enhancements. The model simulations first tested whether reasonable UV enhancements alone could explain the observed OH enhancements in region B. It was found that the observed OH concentrations were most readily explained in this region if UV was enhanced by a factor of about 2 relative to clear-sky conditions. This is a reasonable value given the observed enhancements of up-welling short-wave radiation shown Figure 2f. Another factor contributing to higher OH levels in region B is elevated water vapor concentrations, plotted in Figure 6a. According to the model, the greater water vapor accounted for roughly 25% of the OH enhancement and doubled UV flux contributed roughly 75%. This interpretation is consistent with the measurements of *Mauldin et al.* [1997] who reports that OH concentrations above clouds can be a factor of about 3 times that observed in clear air, and within clouds were 2 times higher than clear air. Note that no significant H_2SO_4 appeared to be produced under the latter conditions, likely due to the H_2SO_4 being scavenged by the high surface area provided by the cloud drops in this region. The characteristic time for H_2SO_4 scavenging by the cloud droplets is 4 min and H_2SO_4 production is not that rapid. For example, without any scavenging it takes roughly 13 min just to produce the observed H_2SO_4 concentrations of 4×10^5 cm^{-3}.

Since up-welling short-wave radiation in the nucleation regions was also higher, a similar UV enhancement in this region is used to calculate OH concentrations and then H_2SO_4 concentrations. However, first, as a base case, a diurnal OH profile was generated assuming no UV enhancement and then an OH profile was generated assuming a factor 2 enhancement. The simulation results are shown in Figures 6b and 6c, respectively.

3.1.3. H_2SO_4 simulations. Diurnal H_2SO_4 concentrations were calculated assuming initial concentrations of 10^4 cm^{-3}, a constant SO_2 concentration at the observed level of ~ 10 pptv and accounting for losses by scavenging and production of new particles. With no UV enhancement H_2SO_4 reaches a peak value of 1.8×10^6 cm^{-3} about 0.5 hour prior to when the measurements were made; see Figure 6b. This is lower then the value of 2.5×10^6 cm^{-3} observed in the nucleation region. In contrast, simulations run with double clear-sky UV intensities produce peak diurnal H_2SO_4 concentrations of 3.1×10^6 cm^{-3}, concentrations that are higher than those observed in the nucleation region (Figure 6c). This suggests that a reasonable UV enhancement of 1 to 2 times clear sky levels could produce the observed H_2SO_4 concentrations. Combined with the trend in the observed H_2SO_4 concentration, the observations and model simulations are consistent with the hypothesis that the enhancement was an isolated and local event brought about by the unique conditions near the frontal cloud.

Model simulations testing the sensitivity of H_2SO_4 concentrations to SO_2 levels show that SO_2 enhancements that are comparable to the observed SO_2 concentrations near the cloud can also explain the peak H_2SO_4 concentrations in the nucleation region. For example, with a constant SO_2 concentration of 17.5 pptv, which is the maximum SO_2 concentration observed in the vicinity of the frontal cloud (see Figure 3), and with no UV enhancement, H_2SO_4 concentrations peak at 3.0×10^6 cm^{-3}. This is comparable to the model simulations where UV was doubled. With doubled UV at these higher SO_2 concentrations, H_2SO_4 reaches a much higher value with a peak concentration of 5.5×10^6 cm^{-3}. Thus reasonable SO_2 enhancement, with no increased OH, could also explain the observed H_2SO_4 concentrations in the nucleation region. Note, however, that lower H_2SO_4 concentrations would be predicted if some depletion of SO_2 was considered in the simulation (e.g., SO_2 not held constant at the elevated level of 17.5 pptv). Thus SO_2 enhancements in the cloud detrainment region due to cloud pumping of surface DMS could also contribute to higher H_2SO_4 concentrations in the nucleation regions.

3.1.4. DMS simulations. Exploratory simulations were also carried out to assess the potential role of DMS oxidation as a

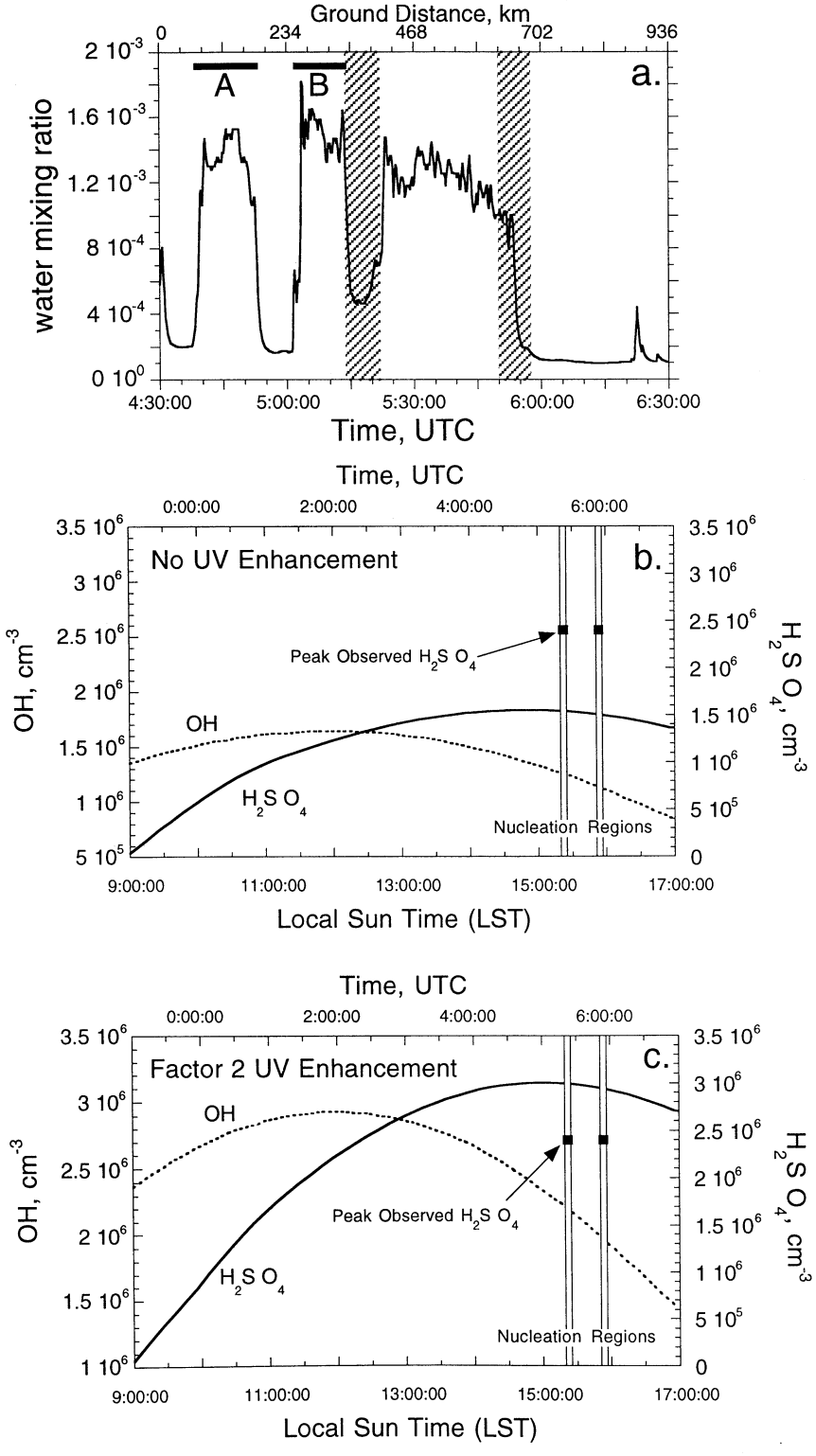

Figure 6. (a) Measured water vapor concentrations used in model simulations to predict diurnal OH levels. (b) Model simulations predicting diurnal OH and H_2SO_4 concentrations based on observed SO_2 at 10 pptv and with no UV enhancement, and (c) with a doubling of UV intensity from reflection from clouds below. For comparison, the plot also shows the maximum observed H_2SO_4 concentrations in the nucleation region.

source of background SO_2 to determine if the observed sulfate particles were of marine origin. At the sampling altitudes of ~ 5.5 km, the DMS photochemical lifetime due to reaction with OH is much shorter than that for SO_2, for clear-sky conditions: 1.1 days versus 20 days [*Berresheim et al.*, 1995]. Thus DMS transported to these altitudes through convection is rather quickly oxidized to form SO_2, which could potentially last much longer than DMS itself. This means the measurements of DMS and SO_2 at a given instant are most likely unrelated because of the large difference in their

photochemical lifetimes. The in situ observations during this flight leg indicated that the levels of SO_2 were in the range of 8 – 18 parts per trillion by volume (pptv), with a median of 10 pptv, while the DMS fell below the limit of detection (LOD). However, even if the DMS levels were, on average, at only half of the LOD value, that is, 0.5 pptv, model simulations suggest that over 7 pptv of SO_2 could be maintained from the DMS oxidation with a yield of 0.75 [*Davis et al.*, 1998, 1999]. Therefore it is possible that these particles were mostly formed from biogenic precursor species (i.e., DMS) emitted at the ocean surface and transported to higher elevations.

3.2. Comparisons of Observations to Binary Nucleation Models

The presence of high 3-4 nm particle concentrations in regions of highest H_2SO_4 concentrations points to H_2SO_4 as a nucleation precursor. An analysis of other measurements of nucleation near clouds has suggested that agreement between predictions of current binary H_2SO_4-H_2O nucleation models and observations improves with increasing altitude [*Weber et al.*, 1999b]. Theory predicts that the binary particle production rate is highly dependent on both precursors, with the relevant parameters being the sulfuric total relative acidity (RA) and the water relative humidity (RH), where RA is the H_2SO_4 vapor pressure (free H_2SO_4 and all monoacid hydrates, that is, our reported H_2SO_4 concentrations) divided by the saturation pressure of pure acid at the ambient temperature. It is noteworthy that although nanoparticles were observed in regions of highest H_2SO_4 (and thus RA, since temperatures were fairly uniform), they were not necessarily found in regions of highest RH. This may indicate that water vapor did not play a pivotal role in nucleation, suggesting an alternative mechanism. We have noted a lack of RH dependence in nucleation regions in other studies where there was strong evidence that binary nucleation was not the mechanism [*Weber et al.*, 1996; *Weber et al.*, 1997; *Weber et al.*, 1995; *Weber et al.*, 1998b].

Comparisons of observed H_2SO_4 concentrations and the H_2SO_4 concentrations necessary for the onset of binary nucleation (1 particle cm^{-3} s^{-1}) according to two binary nucleation models are compared in Table 1. The model of *Jaeker-Voirol and Mirabel* [1989] is commonly used in aerosol simulations in remote marine regions and is included for this reason. The second model, considered to be more accurate, is based on the parameterized [*Kulmala et al.*, 1998] version of the *Wilemski* [1984] model which corrects for a thermodynamic inconsistency inherent in the Jaeker-Voirol and Mirabel model. Laboratory studies [*Ball et al.*, 1999] show that the H_2SO_4 concentration necessary for the onset of nucleation (1 particle cm^{-3} s^{-1}) at relative humidities of 15% and less and at an ambient temperature of 22°C are within a factor of about ±25% of the *Kulmala et al.* [1998]/*Wilemski* [1984] model.

Conditions measured at maximum 3-4 nm particle concentrations for each of the two nucleation regions are compared. The table shows that observed H_2SO_4 concentrations were about a factor of 5 to 10 times lower than that necessary according to the Jaeker-Voirol and Mirabel nucleation model, and factors of 30 to 40 times lower compared to the Wilemski binary model. For the latter case this difference is out of the range of the model uncertainties based on comparisons with experimental results (note that these were at higher temperatures). It should be pointed out, however, that for this study, comparison between measurements and models is difficult for a number of reasons. (1) Because the binary rate is highly sensitive to RH, and RH was changing rapidly in these regions, the comparison depends on the RH chosen. To demonstrate this sensitivity, Table 1 also shows the H_2SO_4 concentration necessary for binary nucleation if the RH is 95%. Under these conditions, observed H_2SO_4 concentrations are sufficient for binary nucleation according to the Jaeker-Voirol and Mirabel nucleation model but not sufficient for nucleation according to the Wilemski binary model. (2) As discussed above, the 3-10 nm particle size distribution suggests nucleation had begun earlier in the day and H_2SO_4 concentrations could have been significantly higher then. The simulations, however, suggest that H_2SO_4 concentrations may have peaked only 0.5 hour prior to the measurements in the nucleation regions and that peak diurnal H_2SO_4 concentrations were not significantly higher than those observed.

A recently developed ternary $H_2SO_4/NH_3/H_2O$ nucleation model can also be used for comparison with the data in the nucleation regions [*Korhonen et al.*, 1999]. This comparison is limited though by the lack of any measurements of NH_3 concentrations and that the model was only run at a lowest temperature of 5°C, whereas the ambient temperatures were

Table 1. Comparison of Observed H_2SO_4 Concentrations and Concentrations Necessary for the Onset of Binary H_2SO_4-H_2O Nucleation in the Two Near-Cloud Regions Where Nucleation Was Observed.

	Region Entering Cloud	Region Exiting Cloud
Time, UTC	0520	0555
Temperature, °C	-22	-24
Relative humidity, %	40	20
Measured H_2SO_4, cm^{-3}	2E6	2E6
H_2SO_4 – H_2O nucleation J-M Model Predicted H_2SO_4, @ ambient RH,[b] cm^{-3}	1E7	3E7
H_2SO_4 – H_2O nucleation W-K model predicted H_2SO_4, @ ambient RH,[c] cm^{-3}	7E7	9E7
H_2SO_4 – H_2O nucleation J-M model predicted H_2SO_4 @ 95% RH,[b] cm^{-3}	2E6	2E6
H_2SO_4 – H_2O nucleation W-K model predicted H_2SO_4 @ 95% RH,[c] cm^{-3}	1E7	1E7

[a] Sulfuric concentrations are in molecules per cm^3.

[b] H_2SO_4 required for a nucleation rate of 1 particle cm^{-3} s^{-1} according to *Jaecker-Voirol and Mirabel* [1989] binary nucleation model.

[c] H_2SO_4 required for a nucleation rate of 1 particle cm^{-3} s^{-1} according to *Kulmala et al.* [1998] parameterization of the *Wilemski* [1984] binary nucleation model.

about –24°C. At H_2SO_4 concentrations of 2 x 10^6 cm^{-3} in the nucleation regions the ternary model predicts that only 10 ppt of NH_3 are necessary for the onset of nucleation. This could be viewed as an upper limit since at lower temperatures, lower NH_3 concentrations are necessary. There is little data on tropospheric NH_3 concentrations, but levels near 10 ppt are not unreasonable [*Warneck*, 1988].

A final point about these data that is perplexing relates to growth rates of the newly formed particles. If only H_2SO_4 and H_2O were condensing onto the freshly formed particles and nucleation had occurred under H_2SO_4 concentrations of about 2 x 10^6 cm^{-3}, it would take over 12 hours for the nucleated particles to reach a detectable size. Since we believe the particles were formed in less than about 6 hours, their growth rates must have been enhanced. Possible mechanisms include condensation of additional species, as proposed in other work [*Weber et al.*, 1997], or by other process, such as ion-induced nucleation and growth [*Turco et al.*, 1998].

In summary, the microphysical mechanisms that produced these nanoparticles are unknown. There is evidence suggesting that H_2SO_4 was involved in nucleation, but there is a discrepancy between the observations and conditions predicted to be necessary for binary nucleation. Ternary mechanisms may be possible but can not be tested rigorously since there were no measurements of NH_3. Finally, the fact that we observed 3 nm particles at such low H_2SO_4 concentrations suggest that the growth of the newly formed particles was greatly assisted by some other species or process.

3.3. Evolution of the Aerosol Size Distributions

It is noted that the aerosol size distribution recorded in the nucleation region near the cloud, shown in Figure 5, has the same characteristic ultrafine particle mode that is often observed at the ocean surface in regions of postfrontal subsidence [*Covert et al.*, 1996]. These measurements support the notion that the distributions observed at the surface evolved from aerosols originally formed near the frontal cloud. The characteristic ultrafine mode observed in the MBL in regions of postfrontal subsidence is probably a result of the dynamics of nucleation near the cloud. It is likely that the ultrafine mode develops and does not merge with larger preexisting particles due to the limited spatial extent of the enhanced vapor concentrations produced in the near-cloud region, combined with the diurnal variation in the photochemical products, which limits nucleation and growth to a single solar day (12 hours). This would result in a finite time for rapid growth of the newly formed particles and sets limits on their final size, thus producing an ultrafine mode with minimum typically in the range of 10 to 20 nm diameter. As the particles are advected away from the cloud and mixed with air of lower condensable vapor concentrations and few nanoparticles, growth slows, the size distribution no longer changes rapidly, and number concentrations decrease.

4. Conclusions

Measurements near a frontal cloud at approximately 6 km above sea level showed evidence of nucleation of new particles exclusively in near-cloud regions. Nucleation was observed in roughly 60 km wide bands that were situated in droplet-free regions of only slightly lower aerosol surface area concentrations but where intensities of up-welling short-wave radiation were significantly enhanced. In the nucleation regions, H_2SO_4 concentrations were ~5 times higher than concentrations recorded farther from the cloud. Particles between 3-4 nm diameter were also observed in the regions of high H_2SO_4 concentrations but were generally not collocated with regions of highest relative humidity along the cloud perimeter. The measurements strongly suggest that H_2SO_4 played a role in nucleation near the cloud. The high UV in the nucleation regions is consistent with the view that this elevated H_2SO_4 was from enhanced photochemistry in these regions. To explore this, a model simulation was performed. It showed that the elevated H_2SO_4 concentrations near the cloud would not be expected unless either OH or SO_2 concentrations were enhanced. In this simple model, UV enhancements of less than 2, due to combined down-welling and up-welling radiation, were sufficient to produce the observed peak H_2SO_4 concentrations. However, we also found that SO_2 enhancements that were reasonable relative to measurements in the general vicinity of the cloud could also explain the higher H_2SO_4 concentrations. The model simulations also suggested that it was possible for the SO_2 to be of marine origin. The observations of nucleation in these regions are not consistent with predictions of binary H_2SO_4-H_2O nucleation models; however, given the limited data set, which did not contain measurements of other possible nucleation precursors, a determination of the particle formation mechanism is not possible.

Acknowledgments. This research is a contribution to the International Global Atmospheric Chemistry (IGAC) Core Project of the International Geosphere-Biosphere Program (IGBP) and is part of the ICAC Aerosol Characterization Experiment (ACE). The authors thank the National Center for Atmospheric Research (NCAR) Research Aviation Facilities (RAF) for the use of their data and NASA for support through grant NAGW-3767.

References

Ball, S.M., D.R. Hanson, F.L. Eisele, and P.H. McMurry, Laboratory studies of particle nucleation: Initial results from the H_2SO_4, H_2O, and NH_3 vapors, *J. Geophys. Res.*, *104*, 23,709-23,718, 1999.

Bates, T.S., B.J. Huebert, J.L. Gras, F.B. Griffiths, and P.A. Durkee, The International Global Atmospheric Chemistry (IGAC) Project's First Aerosol Characterization Experiment (ACE1): Overview, *J. Geophys. Res.*, *103*, 16,297-16,318, 1998.

Berresheim, H., P. Wine, and D. Davis, Sulfur in the atmosphere, in *Composition, Chemistry, and Climate of the Atmosphere*, edited by H. B. Singh, pp. 251-307, Van Nostrand Reinhold, New York, 1995.

Capaldo, K.P., P. Kasibhatla, and S.N. Pandis, Is aerosol production within the remote marine boundary layer sufficient to maintain observed concentrations?, *J. Geophys. Res.*, *104*, 3483-3500, 1999.

Clarke, A.D., Atmospheric nuclei in the remote free-troposphere, *J. Atmos. Chem.*, *14*, 479-488, 1992.

Clarke, A.D., T. Uehara, and J.N. Porter, Atmospheric nuclei and related aerosol fields over the Atlantic: Clean subsiding air and continental pollution during ASTEX, *J. Geophys. Res.*, *102*, 25,281-25,292, 1997.

Clarke, A.D., J.L. Varner, F. Eisele, R.L. Mauldin, D. Tanner, and M. Litchy, Particle production in the remote marine atmosphere: Cloud outflow and subsidence during ACE1, *J. Geophys. Res.*, *103*, 16,397-16,409, 1998.

Clarke, A.D., V.N. Kapustin, F.L. Eisele, R.J. Weber, and P.H. McMurry, Particle production near marine clouds: Sulfuric acid and predicitons from classical binary nucleation, *Geophys. Res. Lett.*, *26*, 2425-2428, 1999.

Coakley, J.A.J., R.D. Cess, and F.B. Yurevich, The effect of tropospheric aerosols on the Earth's radiation budget: A parameterization for climate models, *J. Aerosol Sci.*, *40*, 116-138, 1983.

Covert, D.S., V.N. Kapustin, T.S. Bates, and P.K. Quinn, Physical properties of marine boundary layer aerosol particles of the mid-Pacific in relation to sources and meteorological transport, *J. Geophys. Res.*, *101*, 6919-6930, 1996.

Crawford, J., D. Davis, G. Chen, R. Shetter, M. Müller, J. Barrick, and J. Olson, An assessment of cloud effects on photolysis rate coefficients: Comparison of experimental and theoretical values, *J. Geophys. Res.*, *104*, 5725 - 5734, 1999.

Davis, D., G. Chen, P. Kasibhatla, A. Jefferson, D. Tanner, F. Eisele, D. Lenschow, W. Neff, and H. Berresheim, DMS oxidation in the Antarctic marine boundary layer,Comparison of model simulations and field observations of DMS, DMSO, $DMSO_2$, H_2SO_4(g), MSA(g), and MSA(p), *J. Geophys. Res.*, *103*, 1657-1678, 1998.

Davis, D., et al., Dimethyl sulfide oxidation in the equatorial Pacific: Comparison of model simulations with field observations for DMS, SO_2, H_2SO_4(g), MSA(g), MS, and NSS, *J. Geophys. Res.*, *104*, 5765-5784, 1999.

DeFelice, T.P., and R.J. Cheng, On the phenomenon of nuclei enhancement during the evaporative stage of a cloud, *Atmos. Res.*, *47-48*, 15-40, 1998.

Fouquart, Y., and H. Isaka, Sulfur emission, CCN, clouds and climate: A review, *Ann. Geophys.*, *40*, 462-471, 1992.

Fuchs, N.A., and A.G. Sutugin, Highly Dispersed Aerosols, pp. 47-60, Butterworth-Heinemann, Woburn, Mass., 1970.

Hegg, D.A., Particle production in clouds, *Geophys. Res. Lett.*, *18*, 995-998, 1991.

Hegg, D.A., L.F. Radke, and P.V. Hobbs, Particle production associated with marine clouds, *J. Geophys. Res.*, *95*, 13,917-13,926, 1990.

Jaecker-Voirol, A., and P. Mirabel, Heteromolecular nucleation in the sulfuric acid-water system, *Atmos. Environ.*, *23*, 2053-2057, 1989.

Katoshevski, D., A. Nenes, and J.H. Seinfeld, A study of the processes that govern the maintenance of aerosols in the marine boundary layer, *J. Aerosol Sci.*, *30*, 503-532, 1999.

Knutson, E.O., and K.T. Whitby, Aerosol classification by electrical mobility: Apparatus, theory, and applications, *J. Aerosol Sci.*, *6*, 443-451, 1975.

Korhonen, P., M. Kulmala, A. Laaksonen, Y. Vissanen, R. McGraw, and J.H. Seinfled, Ternary nucleation of the H_2SO_4, NH_3, and H_2O in the atmosphere, *J. Geophys. Res.*, *104*, 26,349-26,353, 1999.

Kulmala, M., A. Laaksonen, and L. Pirjola, Parameterizations for sulfuric acid/water nucleation rates, *J. Geophys. Res.*, *103*, 8301-8307, 1998.

Mauldin, R.L., S. Madronich, S.J. Flocke, F.L. Eisele, G.J. Frost, and A.S.H. Prevot, New insights on OH: Measurements around and in clouds, *Geophys. Res. Lett.*, *24*, 3033-3036, 1997.

Nilsson, E.D., and M. Kulmala, The potential for atmospheric mixing processes to enhance the binary nucleation rate, *J. Geophys. Res.*, *103*, 1381-1389, 1998.

Perry, K.D., and P.V. Hobbs, Further evidence for particle nucleation in clear air adjacent to marine cumulus clouds, *J. Geophys. Res.*, *99*, 22,803-22,818, 1994.

Raes, F., Entrainment of free tropospheric aerosols as a regulating mechanism for cloud condensation nuclei in the remote marine boundary layer, *J. Geophys. Res.*, *100*, 2893-2903, 1995.

Turco, R.P., J. Zhao, and F. Yu, A new source of tropospheric aerosols: Ion-ion recombination, *Geophys. Res. Lett.*, *25*, 635-638, 1998.

Warneck, P., *Chemistry of the Natural Atmosphere, Int. Geophys. Ser.*, vol. 41, Academic, San Diego, Calif., 1988.

Weber, R.J., P.H. McMurry, F.L. Eisele, and D.J. Tanner, Measurement of expected nucleation precursor species and 3 to 500 nm diameter particles at Mauna Loa Observatory, Hawaii, *J. Atmos. Sci.*, *52*, 2242-2257, 1995.

Weber, R.J., J.J. Marti, P.H. McMurry, F.L. Eisele, D.J. Tanner, and A. Jefferson, Measured atmospheric new particle formation rates: Implications for nucleation mechanisms, *Chem. Eng. Commun..*, *151*, 53-64, 1996.

Weber, R.J., J.J. Marti, P.H. McMurry, F.L. Eisele, D.J. Tanner, and A. Jefferson, Measurements of new particle formation and ultrafine particle growth rates at a clean continental site, *J. Geophys. Res.*, *102*, 4375-4385, 1997.

Weber, R.J., A.D. Clarke, M. Litchy, J. Li, G. Kok, R.D. Schillawski, and P.H. McMurry, Spurious aerosol measurements when sampling from aircraft in the vicinity of clouds, *J. Geophys. Res.*, *103*, 28,337-28,346, 1998a.

Weber, R.J., P.H. McMurry, L. Mauldin, D. Tanner, F. Eisele, F. Brechtel, S. Kreidenweis, G. Kok, R. Schillawski, and D. Baumgardner, A study of new particle formation and growth involving biogenic trace gas species measured during ACE 1, *J. Geophys. Res.*, *103*, 16,385-16,396, 1998b.

Weber, R.J., P.H. McMurry, T.S. Bates, D.S. Covert, F.J. Brechtel, and G.L. Kok, Intercomparison of airborne and surfaced-based measurements of condensation nuclei in the remote marine troposphere measured during ACE 1, *J. Geophys. Res.*, *104*, 21,673-21,683, 1999a.

Weber, R.J., P.H. McMurry, L. Mauldin, D. Tanner, F. Eisele, A. Clarke, and V.N. Kapustin, New particle production in the remote troposphere: A comparison of observations at various sites, *Geophys. Res. Lett.*, *26*, 307-310, 1999b.

Wilemski, G., Composition of the critical nucleus in multicomponent vapor nucleation, *J. Chem. Phys.*, *80*, 1370-1372, 1984.

A. R. Bandy and D. C. Thornton, Department of Chemistry, Drexel University, Philadelphia, PA 19104, USA.

G. Chen, D. Davis, F. L. Eisele, and R. J. Weber, School of Earth and Atmospheric Sciences, Georgia Institute of Technology, Atlanta, GA 30332-0340, USA. (rweber@eas.gatech.edu)

A. D. Clarke, School of Ocean and Earth Science and Technology, University of Hawaii, Honolulu, HI 96822, USA.

R. L. Mauldin III and D. J. Tanner, Atmospheric Chemistry Division, NCAR, P. O. Box 3000, Boulder, CO 80303, USA.

(Received October 30, 2000; revised June 20, 2001;
accepted June 27, 2001.)